BWG GEOCHEMISCHE BERATUNG GbR

ZUR UNTERSUCHUNG VON WASSER UND GAS

Report

Geochemical investigations of water and solid samples at Honselersdijk GT 1 during the hydraulic test on 07-08 March 2012

INDEX

LIST OF FIGURES AND TABLES

1. Description of the services

Two gas samples and one water sample of the geothermal well Honselersdijk Gt 1/Netherland during the hydraulic test on 07-08 March 2012 were characterised geochemically. There were determined:

- Gas / water ratio
- Total gas composition
- Components dissolved in the water: anions: chloride, bromide, iodide, fluoride, hydrogen carbonate, sulphate; cations: Li, K, Na, Ca, Mg, NH4, Ba, Fe (tot.), Mn, Sr, Cr, Pb, Cu, Al, Zn, As, Hg, U
- Silica, boron
- pH value (laboratory),
- Density
- Mineralisation
- Dry matter at 180°C
- Determination of in-situ parameters (pH-, Eh values, conductivity, temperature, KS and
- KB values, organoleptic evaluation, rapid determination of solute sulphide)
-

The analysis was done in cooperation with accredited laboratories.

The degassing pressure was calculated from the results of the analysis.

Microfiltration of the geothermal fluid had been conducted 3 hours before (1st sample) and at the end of the hydraulic test (2nd sample) at Honselersdijk Gt 1 on March 8, 2012. The Investigations (analysis and evaluation) of the solids were done by Mr. Birner, Geothermie Neubrandenburg GmbH.

2. Results of the water analysis

After filtration of the samples (0.45 µm), an aliquot of the filtered sample was acidified with HNO_3 for cation analysis. The physico-chemical properties of the samples were analysed and summarised in Table 1 and Table 2.

The fluid produced from the deep well Honselersdijk Gt 1/Netherland was clear water with a pH value of 6.0. The fluid shows reducing conditions. The salt content is approx. 123 g/L.

The sodium content is around 40.0 mEq%. Chloride dominates the anions (49.8 mEq%). Thus, the formation fluid has to be assigned to the Na-Cl type. The contents of calcium (7.3 mEq%) and magnesium (1.9 mEq%) are lower by one order of magnitude. All the other solute components show clearly lower concentrations. The formation fluid contains a lot of iron – approx. 70 mg/L and gets brown after longer standing and contact with oxygen. The sulphate concentration is 200 mg/L; HS- or S^{2-} are undetectable or below the detection limit (<0.2 mg/L).

Table 1: Physico-chemical properties

Denomination		HON GT1-070312	HON GT1-080312	HON GT1-080312
Date of sampling	**unit**	07.03.2012 6:40 p.m.	08.03.2012 1:30 p.m.	08.03.2012 4:30 p.m.
Temperature	°C		85.8	86.1
Production rate	l/s		43.3	43.4
Production amount	m³		3,940	4,250
Parameter				
Colour		light yellow (very low oil film)		
Turbidity		none		
Smell		specific, little like hydrocarbons		
Precipitate		in air brown solids		
Degassing		yes		
Sample temperature	°C	81.3	81.4	83.7
pH value at sample temperature		6.18	6.01	6.01
pH value at 20.0°C		6.20	n.b.	5.96
Redox potential measured for Ag/AgCl	mV	-268	-265	-282
Redox potential SHE	mV	-93	-90	-109
Oxygen (O_2)	mg/l	<1	<1	<1
Conductivity on site	mS/cm	145.0	n.b.	141.7
Conductivity (25°C) at laboratory	mS/cm	165.4	n.b.	166.5
Density 20°C	g/cm³	n.b.	n.b.	1.091
Acid capacity pH 4,3	mmol/L	2.68	n.b.	2.48
Base capacity pH 8,2	mmol/L	5.35	n.b.	5.15
Sulphide	mg/L	undetectable		

Table 2: Chemical composition

	HON-GT1-080312 4:30 p.m.				
		c (m)		c (eq)	
Cations					
Lithium	Li^+	5,28	[mg/L]	0,76	[mEq/L]
Sodium	Na^+	38800	[mg/L]	1687,69	[mEq/L]
Potassium	K^+	458	[mg/L]	11,71	[mEq/L]
Calcium	Ca^{2+}	6190	[mg/L]	308,88	[mEq/L]
Magnesium	Mg^{2+}	983	[mg/L]	80,91	[mEq/L]
Strontium	Sr^{2+}	373	[mg/L]	8,51	[mEq/L]
Barium	Ba^{2+}	8,24	[mg/L]	0,12	[mEq/L]
Iron (tot.)	Fe^{2+}	72,1	[mg/L]	2,58	[mEq/L]
Manganese	Mn^{2+}	1,67	[mg/L]	0,06	[mEq/L]
Ammonia	NH_4^+	76,7	[mg/L]	4,25	[mEq/L]
Total cations		**46968**	[mg/L]	2105	[mEq/L]
Anions					
Chloride	Cl^-	75710	[mg/L]	2135,68	[mEq/L]
Hydrogen carbonate	HCO_3^-	151	[mg/L]	2,48	[mEq/L]
Sulphate	SO_4^{2-}	200	[mg/L]	4,16	[mEq/L]
Nitrate	NO_3^-	<0,50	[mg/L]		
Bromide	Br^-	194	[mg/L]	2,43	[mEq/L]
Iodide	I^-	1,0	[mg/L]	0,01	[mEq/L]
Flouride	F^-	<1,0	[mg/L]		
Total anions		**76256**	[mg/L]	2145	[mEq/L]
Salinity		**123224**	[mg/L]		
Dry matter (180°C)		139300	[mg/L]		
Ion balance	HON-GT1-080312			-39,29	[mEq/L]
Error				-1,85	
Other parameters					
Boron, B		28,0	[mg/L]		
H_3BO_3		160,2	[mg/L]		
Silicon, Si		20,0	[mg/L]		
SiO_2		42,8	[mg/L]		
H_3SiO_3		55,6	[mg/L]		
Trace metals					
Aluminium, Al		6,0	[µg/L]		
Chrome, Cr		11,9	[µg/L]		
Copper, Cu		<7,50	[µg/L]		
Zinc, Zn		372	[µg/L]		
Arsenic, As		6,65	[µg/L]		
Mercury, Hg		<1,00	[µg/L]		
Lead, Pb		8,1	[µg/L]		
Uranium, U		<0,233	[µg/L]		

3. Results of the gas analysis

3.1 Method

Thermal water was taken continuously via an existing „bypass“ and fed into a degasser. The hot thermal water was sprayed in the closed vessel. The gases released in this way are carried away at the head of the degasser.

Figure 1: Degasser at the well Honselersdijk Gt 1

The gas flow was registered over a longer period of time by means of a drum-type gas flow meter and related afterwards to the degassed water (see Figure 2 and Figure 3).

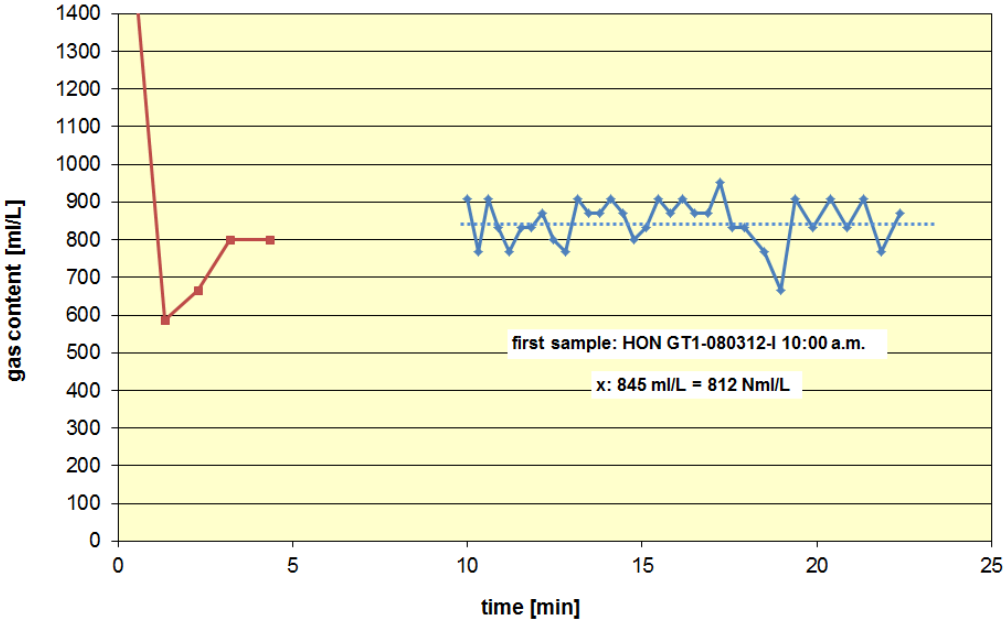

Figure 2: Gas content in one liter fluid vs. the time at a fluid temperature of 75°C (first measurement period on 8th March, 2012 from 8:15 a.m. to 10:00 a.m.)

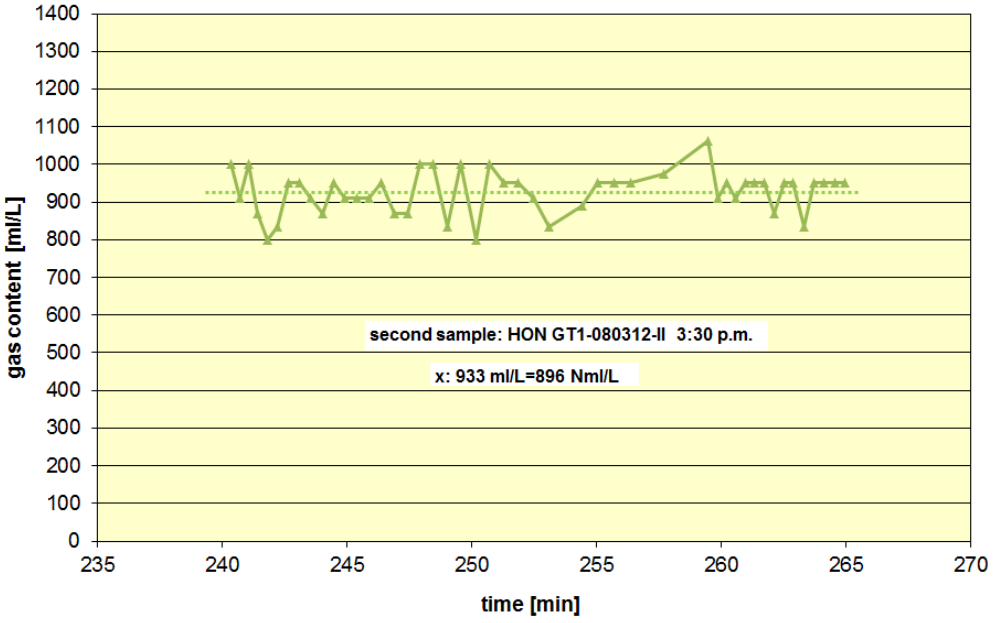

Figure 3: Gas content in one liter fluid vs. the time at a fluid temperature of about 80°C (second measurement period on 8th March, 2012 from 1:45 p.m. to 3:30 p.m.)

3.2 Results

The gas composition was analyzed in the laboratory, observing a stable fluid inflow and outflow after measuring of the gas content. .

Table 3 shows the results of the gas composition. The oxygen in the both samples was very low (around 0.5 vol%).

Table 3: Results of the gas analysis

	HON GT1-080312-I		HON GT1-080312-II	
Date	**08.03.2012**			
Time	**10:00 a.m.**		**3:30 p.m.**	
		calculated O_2-free		calculated O_2-free
Nm^3 (gas)/ Nm^3 (fluid)	**0.812**		**0.896**	
Denomination				
Nitrogen	3.44	1.58	3.17	1.71
Oxygen	**0.51**		**0.4**	
Argon	0.03	0.01	0.02	0.00
Carbon dioxide	8.68	8.90	8.76	8.93
Methane	83.716	85.80	83.997	85.64
Ethene	<0.001	<0.001	<0.001	<0.001
Ethane	2.971	3.04	2.982	3.04
Propene	<0.001	<0.001	<0.001	<0.001
Propane	0.500	0.51	0.499	0.51
i-Butane	0.035	0.04	0.035	0.04
Butene-1	<0.001	<0.001	<0.001	<0.001
n-Butane	0.085	0.09	0.086	0.09
22DMPr	<0.001	<0.001	<0.001	<0.001
i-Pentane	0.014	0.01	0.014	0.01
Pentene-1	<0.001	<0.001	<0.001	<0.001
n-Pentane	0.018	0.02	0.018	0.02
Hexane	0.007	0.01	0.009	0.01
Helium	<0.01	<0.01	<0.01	<0.01
Hydrogen	<0.01	<0.01	<0.01	<0.01

Not all the quantity of carbon dioxide which is dissolved in the fluid under reservoir conditions is degassed at the temperature of 75°C resp. 80°C. That is why the solute carbon dioxide in the water was determined after degassing via the base capacity (KB value up to pH = 8.2). Before the solute iron ions were bonded by means of a sequestrant.

Table 4 gives the results of the two gas samples (air-corrected, standardised) with due consideration of the solute carbon dioxide in the fluid. Under standard conditions (T=273.15 K, p=1.01325 hPa), 1.0 Nm^3 of gas are dissolved in 1 m^3 of fluid. The gas mixture consists mainly of methane. The other hydro carbonates are only 3.3 vol%. The easily soluble gas carbon dioxide is approx. 20 vol%. A little amount of nitrogen (about 1.5 vol%) was analysed.

At the end of the hydraulic test (V=4.250 m³) the gas content is a little higher than that of the first measurement. Also the methane content in one liter fluid is approx. 70 ml more than in sample number one.

Table 4: Results of the gas analysis with dissolved CO_2 in the degassed fluid

Denomination	HON GT1-080312-I	HON GT1-080312-II
Date Time	08.03.2012 10:30 a.m.	08.03.2012 3:30 p.m.
Nm^3 (gas)/ Nm^3 (fluid)	0.93	1.01
Methane, CH_4 Ethane and the other Carbon dioxide, CO_2 Nitrogen, N_2	74.9 vol.-% 3.25 vol.-% 20.4 vol.-% 1.4 vol.-%	76.0 vol.-% 3.30 vol.-% 19.1 vol.-% 1.5 vol.-%

Any further considerations (bubble point) are based on the compositions of the last sample HON GT1-080312-II.

3.3 Determination of the flushing pressure

Solute salts reduce the solubility. The solubility of each gas component in brine can be determined when its solubility in water is known, from equation (1)

(1) $$R_{gas,\ b} = R_{gas,\ w} \cdot \left(\frac{\rho_b - TDS}{1000} \right) \cdot L_{rel.}$$

$R_{gas,\ b}$ gas content of brine [m^3gas/m^3solution]
$R_{gas,\ w}$ gas content of water [m^3gas/ t water]
TDS total dissolved solids [kg salt/m^3 solution]
ρ_b density of brine [kg/m^3]
$L_{rel.}$ relative solubility depending on the salt content of the solution

For the gases N_2 and CH_4, the relative solubility L_{rel} can easily be determined from equation (2) (Harting et al., 1981):

(2) $$L_{rel.} = e^{\left(-0315 \cdot c + 0.01452 \cdot c^2\right)}$$

c molality [mol/kg]

The higher influence of divalent ions on the gas solubility has to be taken into account. This is done by multiplying the molality of $CaCl_2$ by the factor of 1.8 (Harting et al., 1981), which gives an equivalent NaCl concentration causing the same gas solubility reduction. For the molality:

HON GT1-080312-II: 2.14 mol/kg

as determined for the formation water, $L_{rel.}$ is 0.55 referred to pure water ($L_{rel.}$=1).

Carbon dioxide behaves differently from nitrogen, and methane in that dissolved carbon dioxide forms a weak acid. For calculation of the carbon dioxide solubility reduction, there was applied equation 3 (cf. Seibt et al., 1999)

(3) $$S^{CO_2}(T) = \frac{S_0^{CO_2}(T)}{10^{C \cdot 0{,}085}}$$

C	molarity [mol/L]
S	solubility in saline water
S	solubility in pure water.

Accordingly, the solubility of CO_2 in the deep water is only 66.7 % of that in pure water.

HON GT1-080312-II: 66.7% ("NaCl molarity"$_{eq}$ = 2.07 mol/L)

The solubility figures for carbon dioxide, nitrogen, and methane in pure water taken from the literature (Harting et al., 1981) were calculated according to (1) for the thermal water.

According to the mol fraction solubility of the individual gases (carbon dioxide x_{CO2}, methane x_{CH4}, nitrogen x_{N2}) in the mixture

(4) $$x_{CO2} = \frac{n_{CO2}}{n_{CO2} + n_{CH4} + n_{N2}}$$

n_i	amount of the substances [mol]

solubility is related to pressure. The degasssing pressure is determined according to equation (5)

(5) $$P = x_{CO2} \cdot P_{CO2} + x_{CH4} \cdot P_{CH4} + x_{N2} \cdot P_{N2}$$

P	total pressure [MPa]
P_i	partial pressure of the gases [MPa]

Figure 4 shows the pressure-related solubility of the gas mixtures in samples **HON GT1-080312-II** at different temperatures. From correlation of the total gas content of the fluid with pressure – at the respective temperatures – the minimum pressure required to prevent ex-solving of gas is obtained. At p=27 bar

1 Nm³ of gas mixture per litre of fluid remained in solution at a temperature of 85°C (at 90°C: p=28.5 bar).

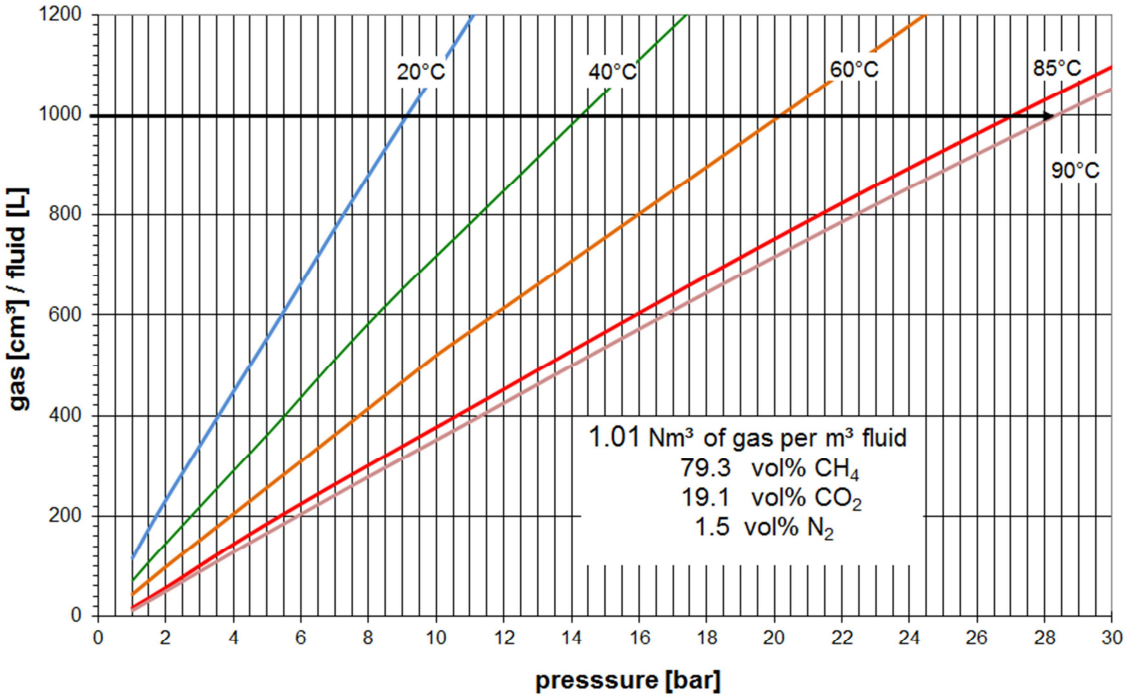

Figure 4: Pressure-related solubility of the gas mixture in sample HON GT1-080312-II at different temperatures

Since the gas mixture consists of carbon dioxide (approx. 20 vol%), the results were checked via the calculation of the degassing of CO_2 depending on pressure and temperature. Several coefficients can be applied as a measure for the solubility of gases. The solubility of CO_2 was done by means of the *Henry constant.* The following empirical relation of the solubility of carbon dioxide in water was derived by Carroll et al., 1991:

(6) $$\ln H_{CO_2} = -6{,}8346 + 1{,}2817 \cdot 10^4 / T - 3{,}7668 \cdot 10^6 / T^2 + 2{,}997 \cdot 10^8 / T^3 \quad (2)$$

applicable at T = 273 up to 433 K and P up to 10 bar

Now, the solubility can be calculated based on the determined H_{CO2} value according to

(7) $$x_{CO_2} \cdot H_{CO_2} = y_{CO_2} \cdot \phi_{CO_2} \cdot P$$

Here, y_{CO2} is the CO_2 mol fraction in the co-existing gas phase, ϕ_{CO2} is the fugacity coefficient for CO_2 in the mixture and P is the total pressure in bar.

$8.9 \cdot 10^{-3}$ mol of carbon dioxide are dissolved per kg of water in the fluid sampled in the well HON GT1. The solubility of CO_2 is shown in Figure 5 for the fluid of the well HON GT1 as a function of temperature under different pressures (after Carroll et al., 1991). According to Figure 5**Fehler! Verweisquelle konnte nicht gefunden werden.**, a pressure of 2 bar under an assumed brine production temperature of 358.15 K is necessary in order to keep the CO_2 concentration in the fluid in solution.

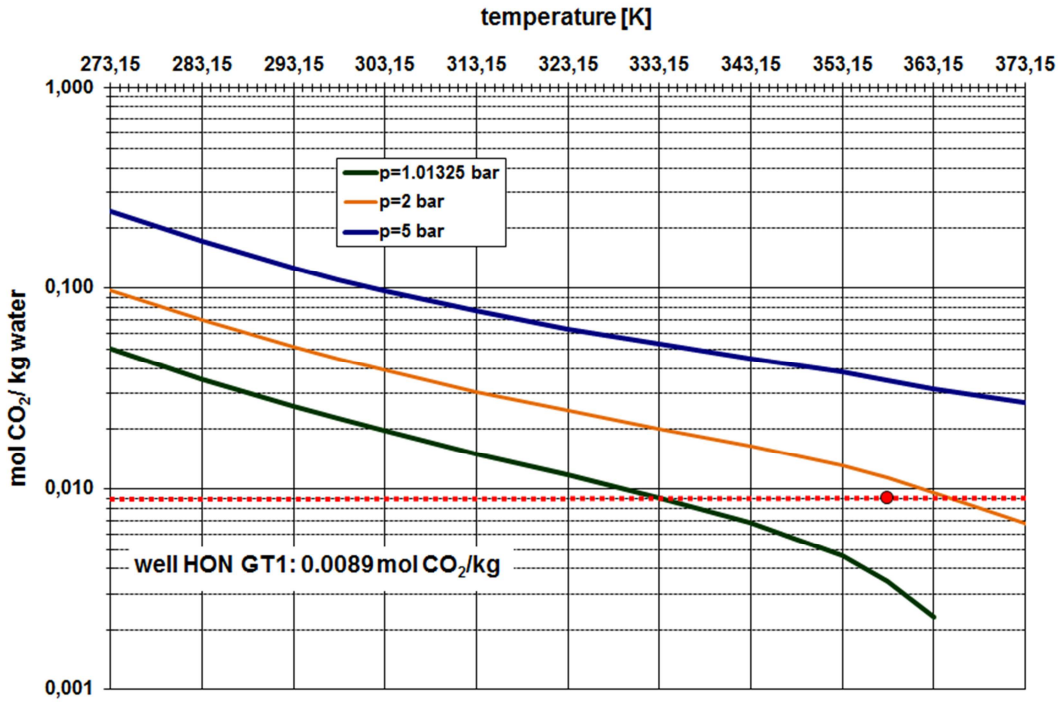

Figure 5: Solubility of CO_2 in brine from HON GT1 well as a function of pressure and temperature (after Carroll et al., 1991)

3.4 Determination of TPH (Total Petroleum Hydrocarbons)

Total Petroleum Hydrocarbons (TPH) - Mineralölkohlenwasserstoffe (MKW) content in the fluid was determined by gas chromatographic (GC). In this application the speed of analysis was detected for the hydrocarbon group eluting between n-Dekan (C_{10}) und n-Tetracontan (C_{40}) with a boiling point between 175°C und 525°C. According to the DIN standard the sample was cleaned by Florisil® before. This cleaning was necessary to adsorb the hydrophilic components on Florisil®.

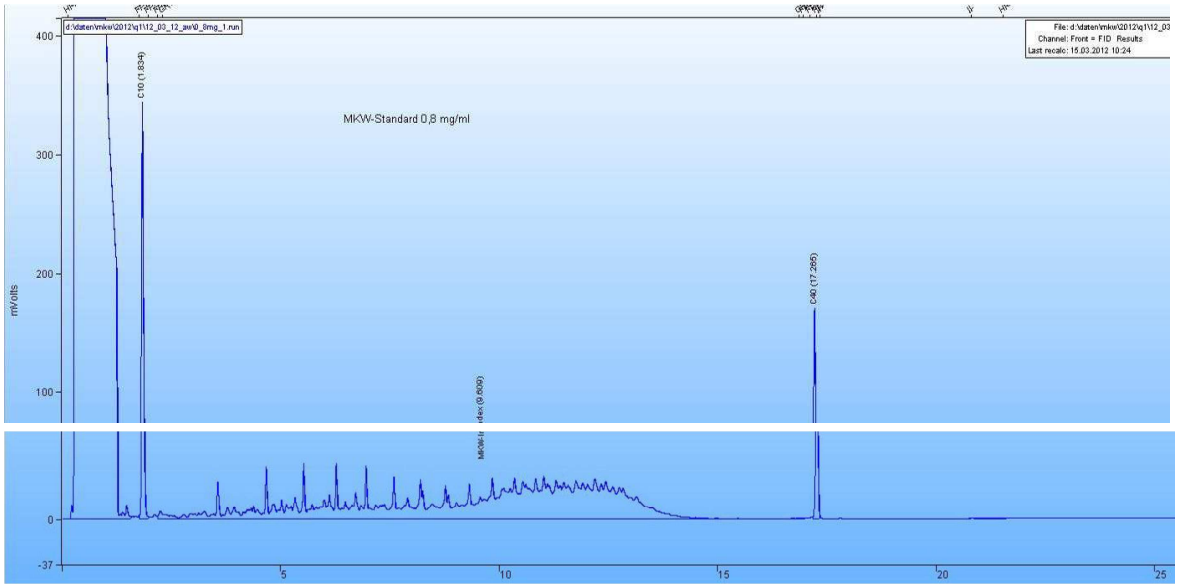

Figure 6: Chromatogram of Total Petroleum Hydrocarbons (TPH) standard in a matrix of diesel fuel and lube oil (0.8 mg/mL)

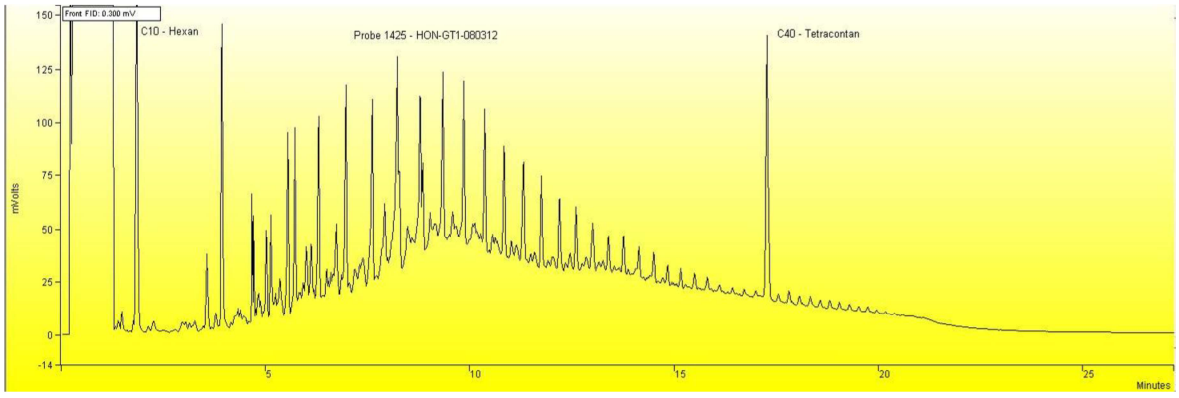

Figure 7: Chromatogram of the sample HON GT1-080312 (05:00 p.m.)

The Total Petroleum Hydrocarbons (TPH) is 2.68 mg/L. The Figure 7 shows good separated hydrocarbons with a medium to high boiling point after the diesel fuel fraction. This proves that the fluid most likely does not contain "casing" fat.

4. Solid sample analysis

4.1 Sampling and field measurements

Microfiltration of the geothermal fluid had been conducted 3 hours before (1st sample) and at the end of the hydraulic test (2nd sample) at Honselersdijk Gt 1 on March 8, 2012 (Figure 8). At each both samples filtration test had been performed by continuously passing water through a 8 micron filter at a constant pressure of 0,5/1 bar and a 0.45 micron filter at a constant pressure of 2,1 bar. During the tests the time required to filter a fixed volume of water is measured to calculate the rate of plugging. Filter curves for the 8 micron filter are shown in in Figure 9 and for the 0.45 micron filter in Figure 10.

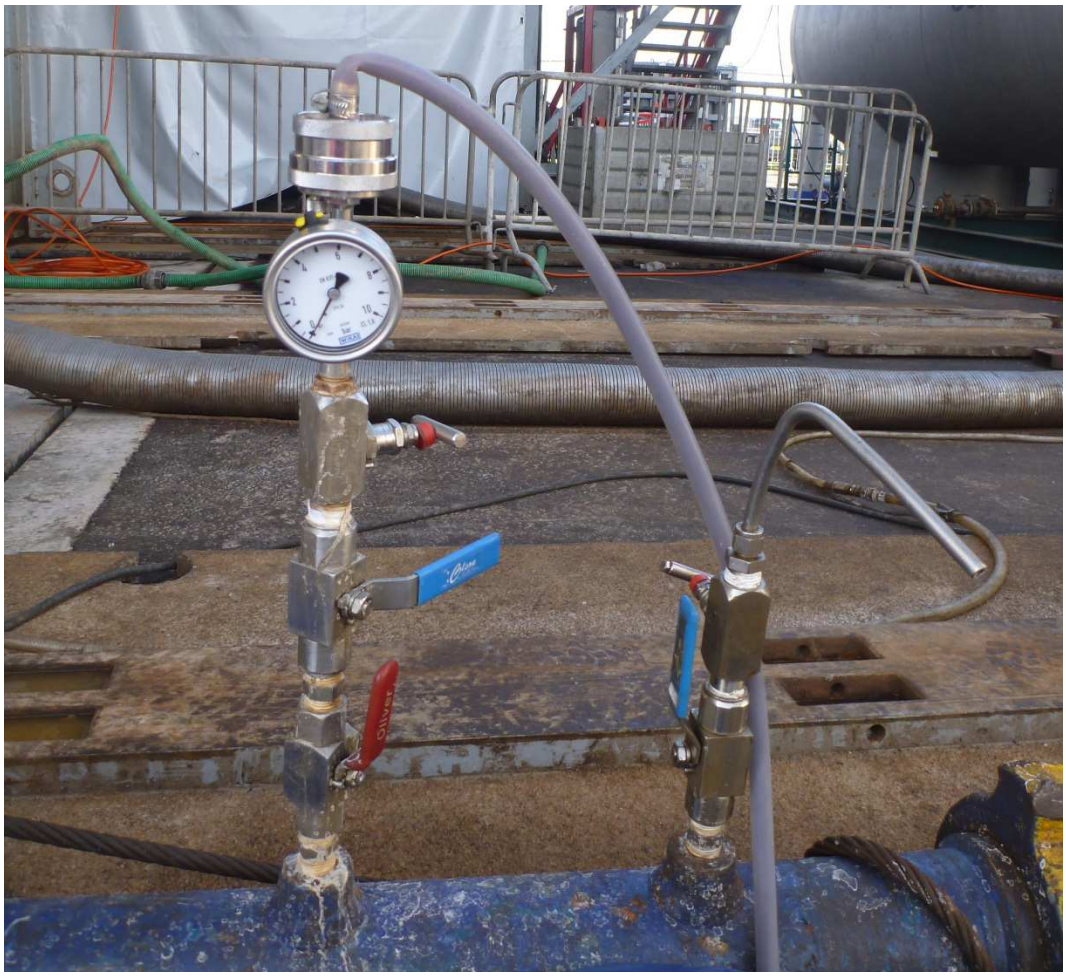

Figure 8: Filtering device at drillsite Honselersdijk consisting of ball values, feed regulator, pressure gauge and a cross flow sampler on top.

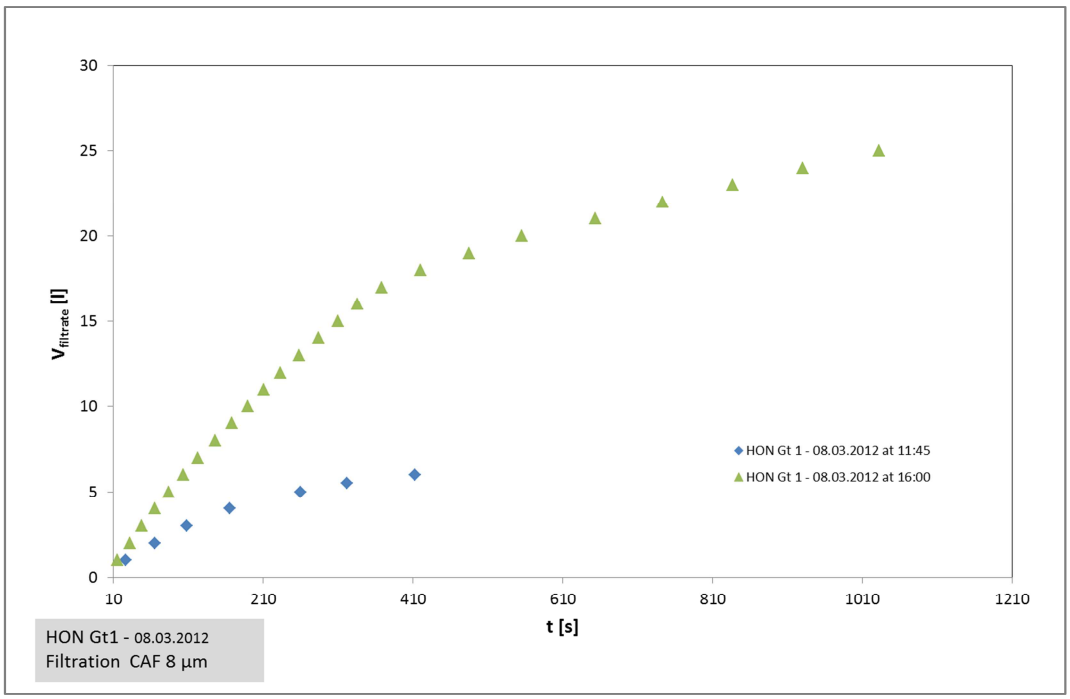

Figure 9: Declining filtrate rate during constant pressure filtration (blue diamonds: 1st sampling with 0,5 bar; green triangles: 2nd sampling with 1 bar) with 8 micron filter

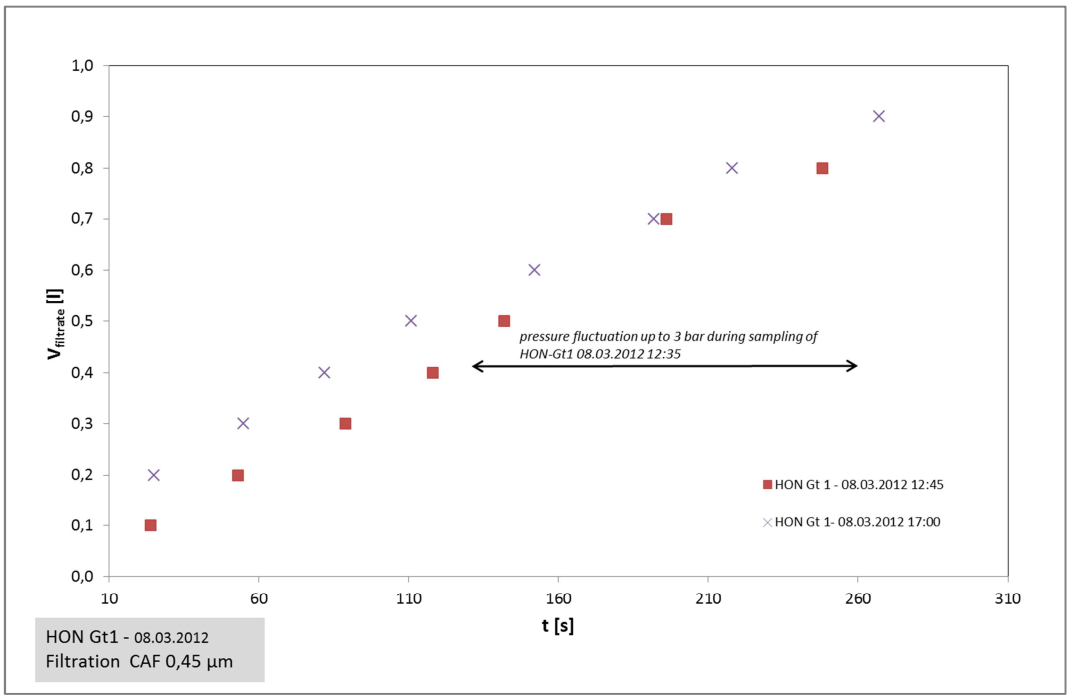

Figure 10: Declining filtrate rate during constant pressure filtration of 2.1 bar (red squares: 1st sampling; purple crosses: 2nd sampling) with 0.45 micron filter.

4.2 Amount of particles in the thermal water

The silt density index (SDI) is a test that attempts to quantify the amount of solid particles in water (ASTM International, 2002). To measure SDI using the standard method, water is passed through a membrane filter at a constant applied gage pressure of 207 kPa (~2.1 bar), and the rate of plugging the filter is measured. The SDI is then calculated from the rate of

plugging using the following equation:

$$SDI_T = \frac{\%\ P_{2,1}}{T} = \frac{[1 - \frac{t_i}{t_f}] \cdot 100}{T}$$

SDI =	Silt density index
T=	test time in minutes between start of first measurement and start of secound measurement [min]
% $P_{2,1}$=	% plugging at 2,1 bar
t_i=	time required to collect initial sample volume [min]
t_f=	time required to collect final sample volume after time T [min]

The results are used to estimate how quickly water will foul a filter membrane. In essence, the SDI test is measuring how quickly silt is built up on a filter, that is, how quickly the filter gets 'plugged' by the silt. The SDI value represents the % plugging per minute of the filter (IWTC 2010).

The modified fouling index (MFI) is determined using the same equipment and procedure used for the SDI. MFI was developed based on Darcy's law, which relates the flux to the thickness of the cake layer (Schippers & Verdouw 1980). The total resistance to flow is the sum of the filter (Rm) and cake resistance (Rc). A change in the flux (dV/dt) is related to the applied pressure (P) through the total resistance (Rm+Rc). Between t/V and V during cake filtration a linear relationship exists. The slope of the linear region is the MFI. A typical filtration curve is shown in Figure 11. The first region represents pore blocking (blocking filtration), the second region represents cake filtration, and the third region represents cake filtration with compression and/or clogging. The slope of the linear region (cake filtration) represents MFI (Adham & Fane 2008).

It has to be distinguished between the MFI of the filtration through an 8 and 0.45 micron membrane filter. Based on the filtration data shown in Figure 12 and Figure 13 the MFI is calculated. At the first sampling MFIs of 4.7 (8 micron filter) and 196.7 (0.45 micron filter) and at the second sampling at the

end of the test MFIs of 0.4 (8 micron filter) and 224.6 (0.45 micron filter) have been calculated. The values indicate a decrease of solids larger than 8 microns and an moderate increase of fine particles in the feed water during the test. It has to be taken into account that the filtration through the 8 micron filter at the first sample had been conducted with a constant pressure of 0.5 bar and at the second test with a pressure of 1 bar. The pressure differences of 0.5 bar leads to 50% overestimation of the decrease of large particles from sampling 1 to 2.

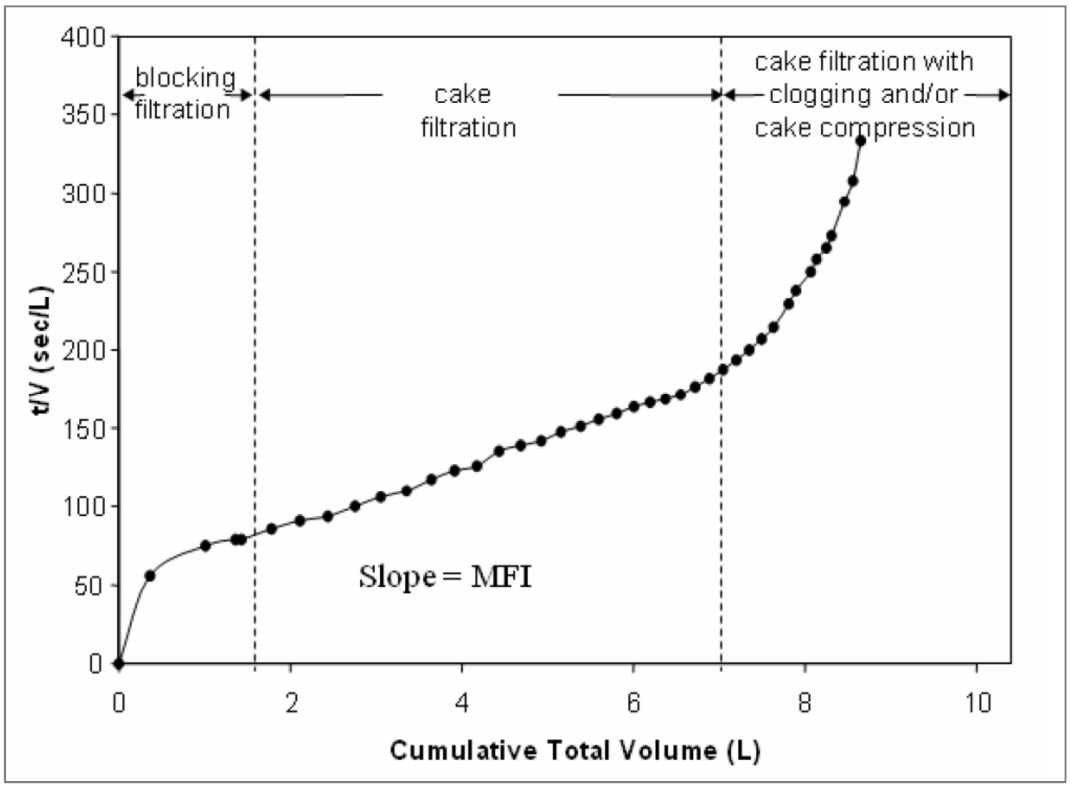

Figure 11: Ratio of filtration and volume as a function of the total volume of filtrated water indicating the three dominant filtration mechanisms (after Adham & Fane 2008).

The SDI values determined after a test time T of 5 minutes (SDI_5) show also a decrease of particles larger than 8 microns (first sample with 8 micron: 17.2; second sample with 8 micron: 13.8). In comparison to the MFI values the decrease of the SDI is moderate. Conversely the increase of fine particles during the test seems to be much higher, if we have look to SDI_5 values of 0.45 micron filtration. From the data of the first sampling a SDI_5 of 5.9 and from the second sampling a SDI_5 of 15.1 can be determined. But the calculation of the SDI_5 of 1st sampling (5.9) is directly influenced by the pressure variations during the filtration and is therefore not representative (Figure 10).

The solid concentrations, obtained from the weight of the cake layer on the membrane filters and the total volume of filtrate, are given in Table 5. The solid concentrations confirm the results of the MFI and SDI analysis. During the test a decrease of particles larger than 8 µm is observed, while the concentration of small particles increases moderately.

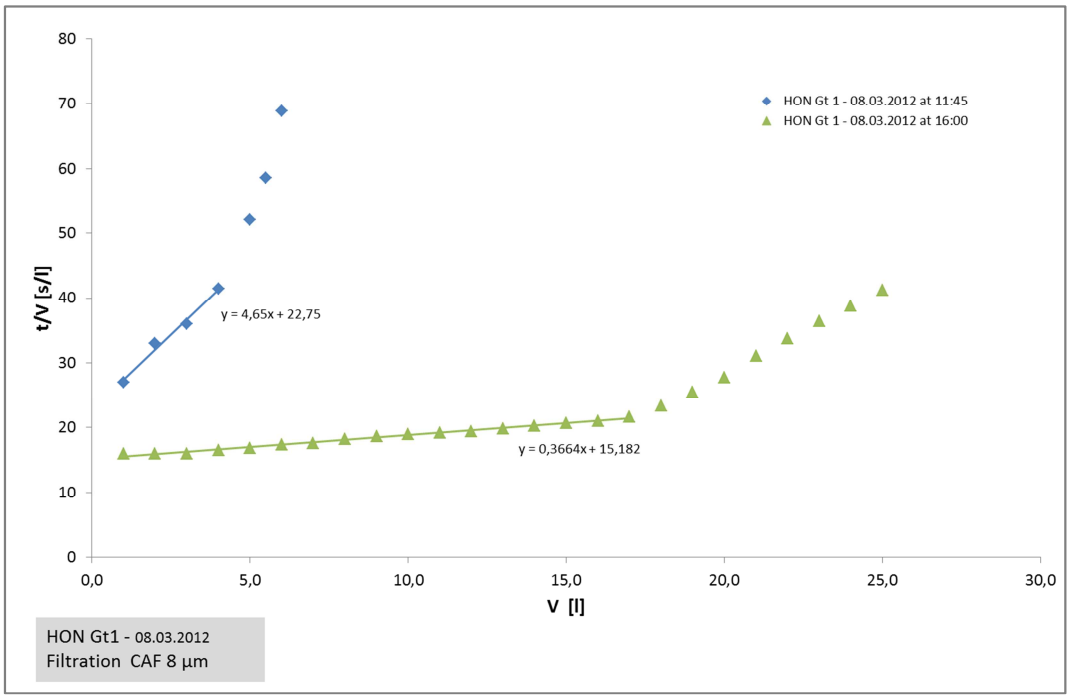

Figure 12: t/V vs V plot of the filtration through a 8 micron filter at 11:45 (1st sampling - blue diamonds) and at 16:00 (2nd sampling - green triangles) on 08.03.2012.

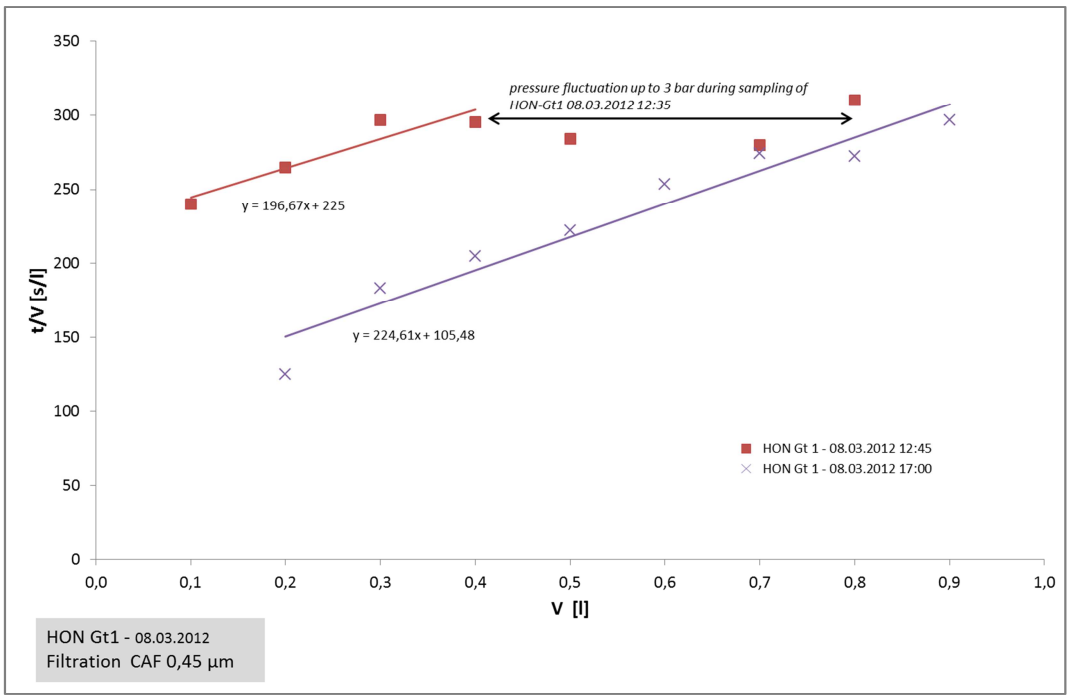

Figure 13: t/V vs V plot of the filtration through a 0.45 micron filter at 12:45 (1st sampling - red squares) and 17:00 (2nd sampling - purple crosses) on 08.03.2012.

Table 5: Amount of particles in water based on MFI, SDI and solid concentrations of filter samples from 08.03.2011

Sampling	Filter type	MFI	SDI5	c [mg/l]
1	CAF 8 µm	4.7	17.2	5.0
	CAF 0.45 µm	196.7	5.9	10.6
2	CAF 8 µm	0.4	13.8	1.5
	CAF 0.45 µm	224.6	15.1	11.0

4.3 Particle size distribution

The particle-size distribution based on sample 2 at the end of the hydraulic test on 08.03.2012 shows that 86.4 % of all solids have diameters in the range of 0.45 to 8 µm (Figure 14). Only less than 4 % of the particles in the thermal water have diameters larger than 100 µm. The median diameter is D_{50}= 2.3 µm, while the maximum particle found has a diameter of 320 µm. The smallest particles have a diameter of 0.45 µm. This is based on a widely used convention that considers particulate matter to be larger than 0.45 µm in diameter. Anything smaller is considered to be dissolved. This boundary is not entirely valid because clay particles and silt can be much smaller than 0.45 µm. For practical purposes,

however, the boundary is convenient, not least because standard membrane filters with 0.45 µm diameter pores can be used to separate suspended particles from dissolved solids.

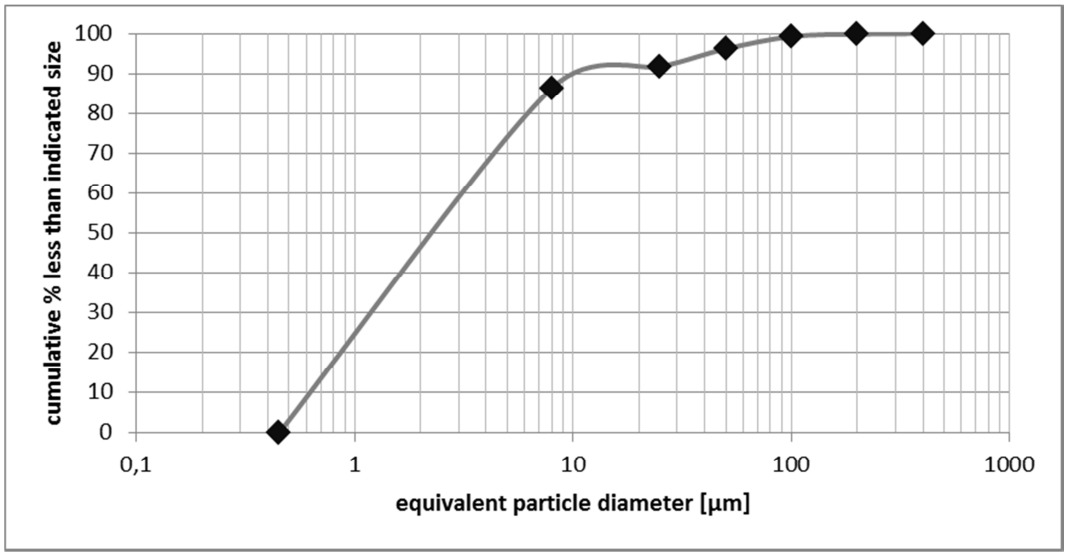

Figure 14: log-normal particle-size distribution of the 2nd sample, based on cake layer analysis of 0.45 & 8 micron filter; Mass medium diameter D_{50}= 2,3 µm

4.4 Composition of particles

The composition of particles of sample 2 (end of test) are analyzed by optical microscopy and SEM-EDX. Optical microscopy analysis provide representative information on particles of diameters larger than 8 µm. Figure 15 illustrates particels on the 8 micron filter as seen under the optical microscope. Photo 15a shows angular to sub rounded, milky quartz grains with a size up to 100 µm in brownish matrix. The black spots represent organic compounds (oil, organic coatings). Material (Fe(OOH)?) from the aquifer can be observed in picture 15b, while picture 15c and 15d show antropogenic materials.

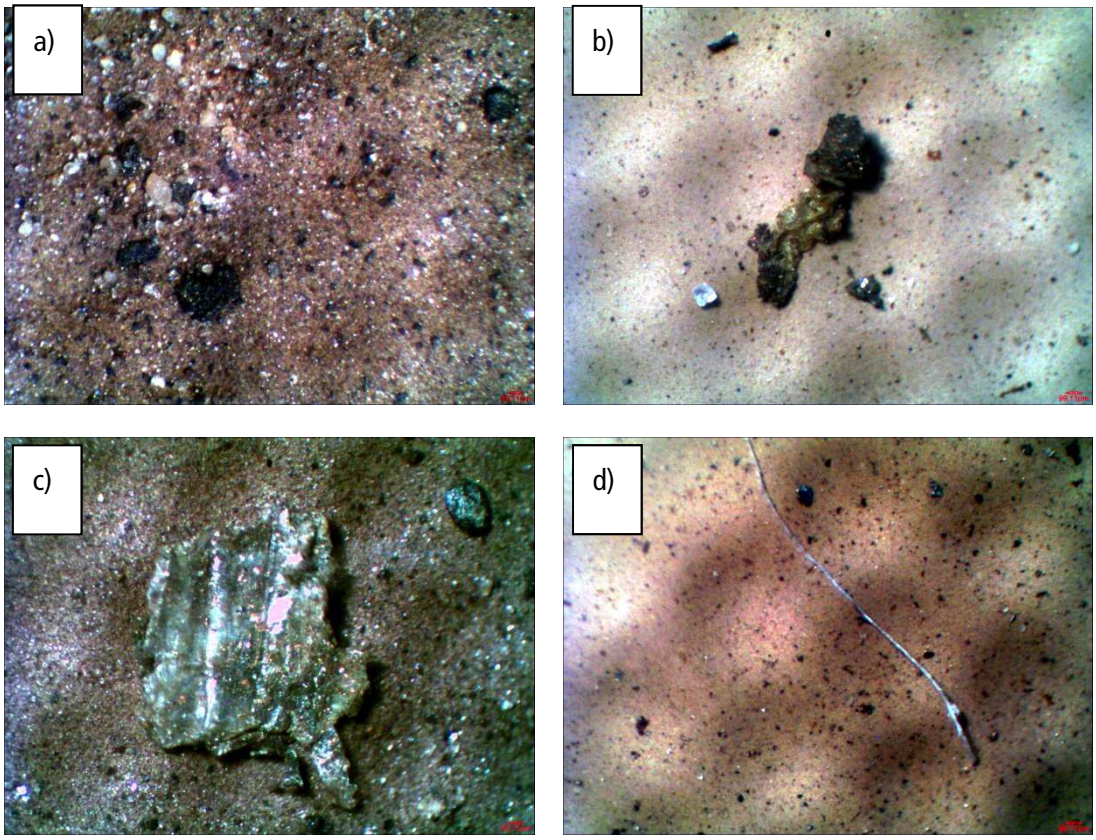

Figure 15: Microscopic images of particles on the 8 micron filter (sample 2). a) milky white quartz grains in brownish matrix, b) brownisch-black aquifer material, c) Steel component (from casing/drill bit), d) white organic fiber

The 0.45 and 8 micron sample were also observed with SEM. Elemental compositions being analyzed by EDX. The EDX analysis reveals that most of the components are quartz (35-40 %) and feldspar (20-25 %). Furthermore iron hydroxides (~15 %), Cu-Zn-(Fe)-oxides (~10 %), Cr-Fe-Ni steel (5 %), CaCO3 (~5 %), FeS_2 (~2 %) and clay minerals are observed (Figure 16).

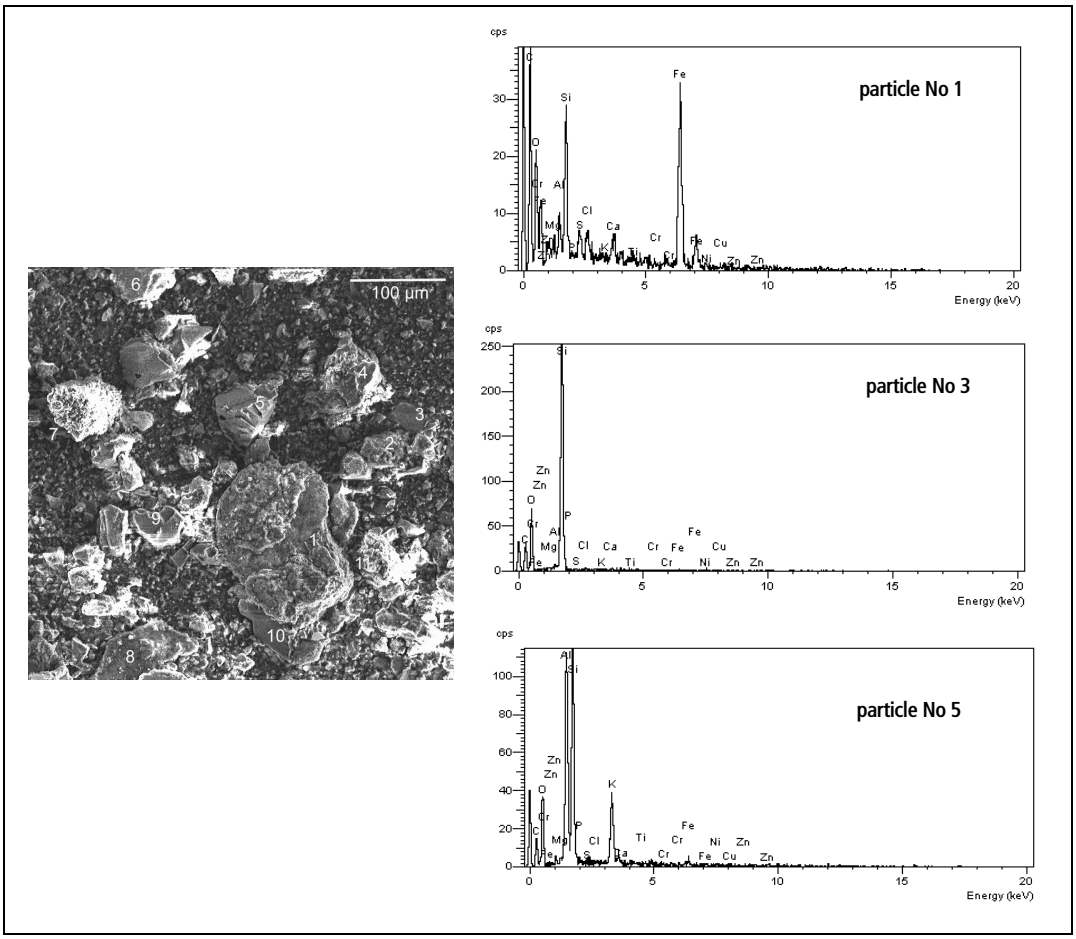

Figure 16: SEM micrograph and corresponding EDX spectra of particles on the 8 micron filter (sample 2). Particle No 1: quartz grain with iron oxide/hydroxide coating; particle 3: quartz grain; particle 5: Potassium feldspar

4.5 Conclusion and recommendations on filter technologies

It can be seen, that during the test a decrease of particles larger than 8 µm was observed, while the concentration of small particles increased moderately. At the end of the hydraulic test on 08.03.2012 86.4 % of all solids had diameters in the range of 0.45 to 8 µm and only 13.6 % had a diameter larger than 8 µm. The median particle diameter is D_{50}= 2.3 µm, while the maximum particle detected had a diameter of 320 µm. Most of the solids found are quartz (35-40 %) or feldspar grains (20-25 %) from the aquifer (or the gravel pack - if applicable). Together with Cu-Zn-(Fe)-oxides and Cr-Fe-Ni steel which indicate that the cleaning of the well had not been completed at the end of the test. A decrease of large particles from 5 mg/l to 1.5 mg/l could be seen during the test, but it is necessary to measure the particle concentration in a further test to obtain information on constant particle load.

From the first results (Q=~35 l/s) we suggest to install bag filters with a mesh size of 10 up to 20 micron at the production well and a 1 micron bag filter system on the injection well. This or similar configurations are widely used in geothermal power plants in the North German basin. It has to be taken into

account, that the observed composition and amount of particles are not representative for the thermal fluid during long term operation. For this reason we recommend a particle monitoring during the next tests to optimize the mesh apertures of the filters.

5. References

ADHAM, S.S., & FANE, A.G. (2008): Cross flow sampler fouling index. NWRI Final Project Report, 22 S., Fountain Valley, CA, USA.

ASTM International (2002): Standard Test Method for Silt Density Index (SDI) of Water, D 4189-95. ASTM International, West Conshohocken, PA.

CARROLL, J.J., J.D. SLUPSKY and A.E. MATHER, (1991): The solubility of carbon dioxide in water at low pressure, J. Phys. Chem. Ref. Data, 20 (6), 1201-1209.

HARTING, P., MAY, F. and SCHÜTZE, H. (1981). Tabellen und Diagramme zur Löslichkeit von Methan-Stickstoff-Gemischen in wässriger Natriumchloridlösung. ZfI-Mitteilungen, Vol. 42, pp. 1-427.

IWTC (2010): Industrial Water Treatment Consulting (2010): SDI - Silt density index – examined and explained. - 7p.

SCHIPPERS, J.C. & VERDOUW J. (1980): The Modified Fouling Index. A Method of Determining the Fouling Characteristics of Water. Desalination, 32: 137-148.

SEIBT, A., NAUMANN, D. and HOTH, P., (1999): Lösung und Entlösung von Thermalwassergasen – Konsequenzen für den Anlagenbetrieb, in: Geothermie Report 99-1: Geothermisches Heizwerk Neustadt-Glewe: Zustands- und Stoffparameter, Prozeßmodellierungen, Betriebserfahrungen und Emissionsbilanzen, Herausgeber: Schallenberg, K., E. Huenges, K. Erbas und H. Menzel, GeoForschungsZentrum Potsdam, Scientific Technical Report, STR99/04, 63-86.